Patient-Specific Contact Mechanics for Anatomic and Reverse Shoulder Arthroplasty using Finite Element Modeling

Brendan M. Curran, Kevin B. Shelburne, Chadd W. Clary, Casey A. Myers
University of Denver, Denver, CO

Disclosures: Brendan M. Curran (N), Kevin B. Shelburne (N), Chadd W. Clary (N), Casey A. Myers (N)

INTRODUCTION: While the two major forms of total shoulder arthroplasty (TSA) continue to rise in usage [1], revision rates remain high (anatomic TSA (aTSA): 5.6%, reverse TSA (rTSA): 2.5%) relative to the hip and knee, with glenoid component loosening in aTSA and joint instability in rTSA causing 34.7% and 38.5% of all revisions, respectively [2]. Joint center repositioning and component alignment after TSA result in changes to muscle force production and glenohumeral (GH) joint loading [3]. Differences in joint forces may contribute to loosening in aTSA and instability in rTSA [4]. Finite element (FE) models can describe component contact pressure and stability in TSA, yet most FE models do not account for patient-specific kinematics and muscle-driven joint forces [5]. The purpose of this study was to develop patient-specific FE models driven by each patient's kinematic profile and joint reaction forces computed by patient-specific musculoskeletal (MSK) models, to compare centers of pressure (COP) and stability ratios (SR). Quantifying COP and SR while accounting for unique anatomy and motion patterns can inform optimal implant placement in individual patients.

METHODS: Patient-specific FE models of the glenohumeral joint were developed in Abaqus Explicit (2020) for TSA patients (5 male, 1 female. 3 aTSA, 3 rTSA, mean age: 76±5 years (range: 71-84 years), mean mass: 100.0±15.3 kg, mean height: 1.7±0.9 m). Humerus and scapula implant geometries were modeled as rigid bodies during FE analysis with polyethylene-titanium contact modeled using a calibrated pressure-overclosure relationship [6]. Abduction and flexion movements (Fig. 1A) were simulated. All rotational DOF of the humerus geometries were driven in displacement control to match 3DOF rotational kinematic data from high-speed stereo radiography (HSSR) (Fig. 1B), while all translational DOF were driven in force control according to loads derived from previously developed patient-specific MSK models using the same HSSR data (Fig. 1C). Custom scripts were used to extract contact pressure contours for the polyethylene component for each implant type (Fig. 1D, 1E). COP locations for each patient were normalized to the AP width and SI height of the polyethylene component of their implant, where values of 100% represent the anterior and superior edges of the implant. AP (anterior +) and SI (superior +) SRs were calculated in the glenoid component coordinate system, which represent the ratio of shear to compressive reaction force. Potential for dislocation increases as values move further from zero [7]. COP, SR, max contact pressure, and contact area means and standard deviations were calculated at discrete poses from the lowest (15 degrees) to highest (60 degrees) common GH elevation values within patient groups, as well as at each patient's final pose (max elevation).

RESULTS: At 60° GH elevation in aTSA glenoid components, normalized AP location of the COP was 49±7% anterior in abduction and 41±25% posterior in flexion (Fig. 2A) relative to the center of the implant; in rTSA humeral components, normalized SI location of the COP was 25±7% inferior in abduction and 53±5% inferior in flexion (Fig. 2B) relative to the center of the implant. In aTSA shoulders, AP stability ratios were 0.26±0.05 in abduction and -0.20±0.13 in flexion (Fig. 3A); in rTSA shoulders, SI stability ratios were 0.40±0.09 in abduction and 1.2±0.11 in flexion at 60° elevation, and were comparable at maximum elevation (Fig. 3B). In aTSA, max contact pressure was slightly greater and contact area was slightly lesser in abduction than flexion at 60° GH elevation (abduction: 6.68±0.74 MPa, 146.1±12.5mm^2, flexion: 6.84±1.41 MPa, 124.2±14.6 mm^2) with larger differences at max elevation (Fig. 3C). In rTSA, max contact pressure was greater and contact area was lesser during flexion than abduction at 60° GH elevation (abduction: 1.15±0.29 MPa, 1167.3±88.9mm^2, flexion: 2.16±0.82 MPa, 602.6±145.7 mm^2, with smaller differences at max elevation (Fig. 3D).

DISCUSSION: In rTSA, SRs and max contact pressure were larger and contact area was smaller during flexion than abduction at 40 and 60° elevation, indicating a higher risk of instability at these elevations, but comparable risk at each patient's maximum elevation. SRs were generally low in aTSA, but the locations of the COP during flexion and abduction were near the anterior (abduction) and posterior (flexion) glenoid edges, suggesting potential for component loosening, particularly at max elevation due to increased pressure and decreased contact area. There was substantial variation between patients in COP and SR values, emphasizing the need for patient-specific FE models to predict implant performance.

SIGNIFICANCE: Patient-specific FE models including joint alignment from CT imaging and driven with kinematics from HSSR and joint loads from accompanying patient-specific MSK models can be used to inform implant placements that minimize the risk of glenoid loosening and instability for various activities in individual aTSA and rTSA patients.

REFERENCES: *[1]* Cecora *et al., JSES Int., 2024; [2]* Parada *et al., J. Shoulder Elbow Surg., 2021; [3]* Curran *et al., J. Biomech. Eng., 2025; [4]* Karelse *et al., J. Shoulder Elbow Surg., 2015; [5]* Stadecker*, JSES Int., 2024; [6]* Fitzpatrick*, J. Biomech. Eng., 2010; [7]* Yanagawa*, J. Biomech. Eng., 2008*

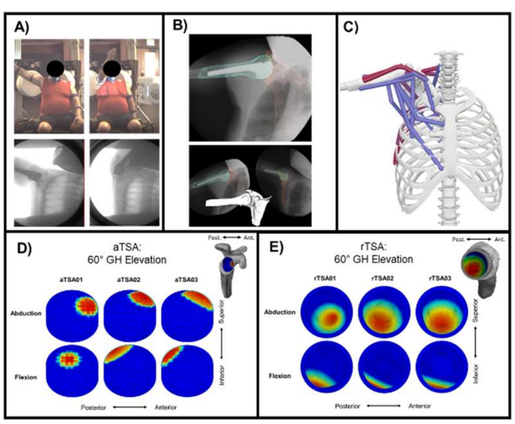

Figure 1: A) patient data collection of abduction (left) and flexion (right) B) Scapula and humerus model-based object tracking of HSSR data using joint geometries from CT data C) OpenSim musculoskeletal model development D,E) FE model contact pressure of aTSA glenoid components and rTSA humeral components at 60° GH elevation

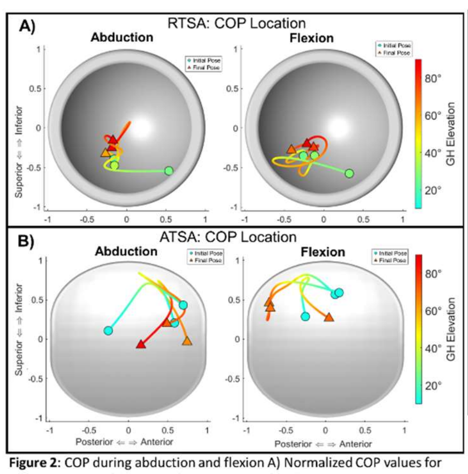

Figure 2: COP during abduction and flexion A) Normalized COP values for A) aTSA patients (n=3) and B) rTSA patients (n=3)

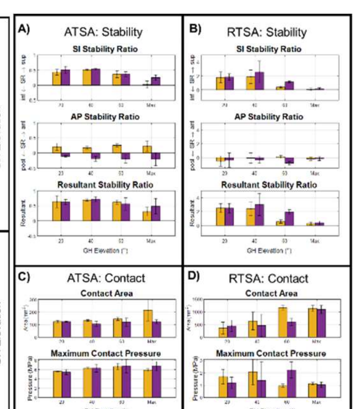

Figure 3: SI, AP, and resultant stability ratios for A) aTSA and B) rTSA patients during abduction and flexion. Contact area and contact pressure for C) aTSA and D) rTSA patients